ARPN Journal of Engineering and Applied Sciences

www.arpnjournals.com

THE APPLICATION OF REMOTE SENSING TECHNOLOGY TO INVESTIGATION OF AREAS BURNED BY FOREST FIRES

Chaiphat Plybour[1,2] and Teerawong Laosuwan[1,2]
[1]Department of Physics, Faculty of Science, Mahasarakham University, Maha Sarakham, Thailand
[2]Space Technology and Geoinformatics Research Unit, Faculty of Science, Mahasarakham University, Maha Sarakham, Thailand
E-Mail: chaiphat.p@msu.ac.th

ABSTRACT

Forest fires once get started cause huge damage. In Thailand, most forest fires are caused by human activities, most likely found in the dry season. This study aims to apply remote sensing technology based on data from Landsat 8 OLI satellite to investigate areas burned by forest fires in Doi Suthep-Pui National Park, Chiang Mai province, Thailand. Differences of spectral indices in 4 patterns are used, i.e. Normalized Difference Vegetation Index (NDVI), Normalized Burned Ratio (NBR), and Burn Area Index (BAI) in April 2021. How the study was conducted included 1) collecting data from Landsat 8 OLI satellite, 2) analyzing the difference of spectral indices in 4 patterns, i.e. NDVI, BAI, and NBR, and 3) analyze data accuracy using statistical methods. The study results revealed that BAI gave the most accurate data for investigating areas burned by forest fires, Kappa Statistics shown was 0.87, followed by NDVI showing Kappa Statistics equal to 0.77, and NBR showing Kappa Statistics equal to 0.67.

Keywords: remote sensing, electromagnetic wave, digital image processing, spectral indices.

Manuscript Received 24 January 2023; Revised 25 June 2023; Published 30 June 2023

INTRODUCTION

Forest fires are the major cause that destroys forest areas in a fast manner. They destroy the balance of an ecosystem tremendously. The main effect of forest fires is the immediate loss of wild animals, including a temporary or permanent loss of forest structure. Each time forest fires shall destroy young plants, making them lose a chance to grow up as big trees. Big trees will stop growing since their wood is deteriorating. Fertile forests finally shall become bare areas (Linta *et al*., 2021). In addition to forest degradation and air pollution, forest fires also impact water resources (Department of National Parks, Wildlife and Plant Conservation, n.d.). Namely, flood, flash flood, landslide, and drought. Moreover, forest fires are the major cause that destroys carbon sinks, places that absorb more carbon than they release, giving rise to the greenhouse effect climate change that has a huge impact on humans. Consequently, forest fires are a problem that must be solved with everyone's cooperation to reduce all direct impacts on humans (Ruthamnong, 2019). According to the report of Forest Fire Control, Department of National Parks, Wildlife and Plant Conservation on statistics of forest fires in Thailand, most of them came from human activities consisting of hunting and gathering wild animals and forest products, burning of agricultural areas, carelessness, and aggravated arson by people in the area (Department of National Parks, Wildlife and Plant Conservation, 2019).

Chiang Mai province in Thailand (where Doi Suthep-Pui National Park is located) has natural forests and mountains approximately 70% of its land area. There are granite and Limestone Mountains covered by various types of forests, such as hill evergreen forests, seasonal rain forests, mixed forests, and deciduous mixed pine-forests rest. Forest areas consist of natural forests, forestry plantations, and naturally recovering forests (Chiang Mai Provincial Office, 2021). Forest areas decline by 0.02% every year due to deforestation, forest fires, etc. Forest fires are more likely to occur in the northern region of Thailand every year, during the drought season from November to April. Most of the forest fires occur in deciduous forests, mixed forests, and forestry plantations. As a consequence, firebreaks should be constructed in many areas and people must give cooperation in stopping the burning of forests to reduce the severity of smoke from forest fires (Kongmeesup, 2020).

Remote sensing technology consists of physics basic principles of electromagnetic waves as a medium to acquire information without direct exposure to an object in 3 patterns, i.e. 1) Spectral, 2) Spatial, and 3) Temporal (ESA, 2016; Elachi & Zyl, 2021; University of Lucknow, n.d.). Using remote sensing technology to collect data from a satellite has an advantage over ground-based field surveys in terms of lower cost. Therefore, it is broadly applied to studies on natural resources and environment (Laosuwan *et al*., 2016; Rotjanakusol & Laosuwan, 2018; Rotjanakusol & Laosuwan, 2019; Rotjanakusol & Laosuwan, 2020; Prohmdirek *et al*., 2020; Jomsrekrayom *et al*., 2021, Suriya *et al*., 2021). In the past investigation and classification of burned areas could be performed using ground-based field surveys. Later, remote sensing technology was applied to collect data from a satellite together with spectral indices, such as Normalized Difference Vegetation Index (NDVI), Burned Area Index (BAI), and Normalized Burned Ratio (NBR) to study areas where forest fires occur (Keeley, 2009; Filipponi, 2018; Rotjanakusol & Laosuwan, 2019; Uttaruk *et al*., 2022). According to the importance mentioned earlier, the objective of this study is the application of remote sensing technology to investigation of areas burned by forest fires in Doi Suthep-Pui National Park based on data obtained

ARPN Journal of Engineering and Applied Sciences

from Landsat 8 OLI and difference of spectral indices, i.e. NDVI, BAI, and NBR April 2021.

STUDY AREA

Doi Suthep-Pui National Park is located in the areas covering Mueang District, Mae Rim District, and Hang Dong District of Chiang Mai Province. It occupies a total area of 261 km^2. The highest peak of the National Park is known as Doi Pui, 1,685 meters above sea level. This National Park comprises fertile forest areas. Though it is located very close to downtown Chiang Mai, most of its forests are in intricately high mountains. Important mountains are Doi Suthep, Doi Pui, etc. Doi Suthep-Pui National Park is characterized by complex features and high cliffs, in the line of Thanon Thongchai mountain range linking to the Himalayas. The elevation of the area ranges between 330 - 1,685 meters above sea level and Doi Pui is the highest peak. The average temperature throughout the year is 2 - 23 ºc, average annual rainfall is 1,350 - 2,500 mm. The average number of rainy days is 139 days. The average annual relative humidity is 70-80%. The weather at the highest peak, Doi Pui, is cold, cool, and humid since it receives vapor from clouds and fog that cover the mountain throughout the year. The lowest temperature in the area is 10-12 ºc during December - February. On the coldest day, the temperature may decrease to 4-5 ºc (Thai National Parks, 2022).

MATERIALS AND METHODS

Data Collection

Landsat 8 OLI is an American Earth observation satellite. The Landsat 8 mission was a collaboration between the National Aeronautics and Space Administration (NASA) and the United States Geological Survey (USGS). It was launched into orbit on 11 February 2013. It has a sun-synchronous orbit and visits the same sport every 16 days. Landsat 8 OLI/TIRS carries two sensors; Operational Land Imager (OLI) and Thermal Infrared Sensor (TIRS), and 11 bands (Table-1) (U.S. Geological Survey, 2020). This study employed data from Landsat 8 OLI during April (the period when forest fires occur every year) in April 2021 as a case study.

Table-1. Landsat-8 operational land imager and thermal infrared sensor.

Bands	Wavelength (µm)	Resolution (m)
Band 1 - Coastal aerosol	0.43-0.45	30
Band 2 - Blue	0.45-0.51	30
Band 3 - Green	0.53-0.59	30
Band 4 - Red	0.64-0.67	30
Band 5 - Near Infrared (NIR)	0.85-0.88	30
Band 6 - SWIR 1	1.57-1.65	30
Band 7 - SWIR 2	2.11-2.29	30
Band 8 - Panchromatic	0.50-0.68	15
Band 9 - Cirrus	1.36-1.38	30
Band 10 - Thermal Infrared (TIRS) 1	10.6-11.19	100
Band 11 - Thermal Infrared (TIRS) 2	11.50-12.51	100

Digital Number (DN) Conversion

This is an important step made before the data from the satellite is analyzed by different indices. DN value was converted to reflectance by equation 1. The obtained data were adjusted by the sun elevation angle calculator as seen in equation 2 (Laosuwan & Uttaruk, 2014; Rotjanakusol & Laosuwan, 2018).

$$L_\lambda = M_L Q_{cal} + A_L \quad (1)$$

Where;

M_L = Radiance Multi Band

A_L = Radiance Add Band

Q_{cal} = Digital Number (DN)

$$\rho_\lambda = M_\rho Q_{cal} + A_\rho \quad (2)$$

Where;

M_ρ = Reflectance Multi Band of Landsat 8 OLI

A_ρ = Reflectance Add Band of Landsat 8 OLI

Q_{cal} = Digital Number (DN)

Analysis of Multi-Temporal Spectral Indices

Spectral indices selected in this study are as follows:

Normalized Difference Vegetation Index (NDVI)

NDVI (Rouse, 1973; Rotjanakusol & Laosuwan, 2018; Rotjanakusol & Laosuwan, 2020) is a dimensionless index that describes the difference between visible and near-infrared reflectance of vegetation cover. The

ARPN Journal of Engineering and Applied Sciences

difference in surface reflectance between – the near-infrared (NIR) wavelength range and the red wavelength range to make is brought to create a proportion with positive values of both wavelength ranges to adjust to being normal distribution (equation 3). The value range of the NDVI is -1 to 1. NDVI close to 1, there is a high possibility that it is dense green leaves but when NDVI is close to zero, there are likely no green leaves. Impacts caused by forest fires give rise to deteriorated forests. NDVI values in forfire-burnedrned areas are usually low or negative.

$$NDVI = (NIR-RED)/(NIR+RED) \quad (3)$$

Where;
NIR = Correspond to the reflectance of band 5 (0.85-0.88 µm) of Landsat 8 OLI
RED = Correspond to the reflectance of band 4 (0.64-0.67 µm) of the Landsat 8 OLI

Burn Area Index (BAI)

BAI (Filipponi, 2018) (equation 4) index highlights burnt-out areas in the red to near-infrared spectrum, by emphasizing the cinder signal in the image after the fire. The index is calculated from the spectral distance from each pixel to the reference spectral point, where the area that has just burned will converge. Brighter pixels represent burned areas.

$$BAI = 1/(0.1-RED)^2+/(0.06+NIR)^2 \quad (4)$$

Where;
NIR = Correspond to the reflectance of band 5 (0.85-0.88 µm) of Landsat 8 OLI
RED = Correspond to the reflectance of band 4 (0.64-0.67 µm) of the Landsat 8 OLI

Normalized Burn Ratio (NBR)

NBR (Keeley, 2009; Xiao *et al*., 2019) is an index used to identify burned areas and provide a measure of burn severity. It is calculated as a ratio between near-infrared (NIR) and short-wave infrared (SWIR) as seen in equation 5. Vegetation has high reflectance in the NIR range and low reflectance in the SWIR range. On the contrary, after a forest fire, vegetation in burned areas has low reflectance in the NIR and high reflectance in the SWIR. Generally, a high NBR value indicates little to no live vegetation exits and bare land and burned areas.

$$NBR = (NIR-SWIR)/(NIR+SWIR) \quad (5)$$

Where;
NIR = Correspond to the reflectance of band 5 (0.85-0.88 µm) of Landsat 8 OLI
SWIR = Correspond to the reflectance of band 7 (2.11-2.29 µm) of the Landsat 8 OLI

Analysis of False Color Composite (FCC)

In this study, FCC is made to investigate the accuracy of forest fire burned areas using data from Landsat 8 (7 (R), 5(G), 4(B)). FCC can indicate burned areas appearing in different shades as follow (Uttaruk *et al*., 2022); Forest fire burned areas appear in purple to dark purple, areas with active fire appear in orange to red, forest areas appear in green or dark green, deciduous forest areas appear in light purple, pink and white, open land appears in white, pink and light orange, agricultural areas appear in white, light green and dark green, and areas for sources of water appear in dark blue.

Accuracy Investigation

Kappa statistic was used to investigate accuracy. The result analyzed by the FCC method was compared point by point using visual interpretation to the results from the analysis of spectral indices (NDVI, NBR, and BAI) in April 2021. In this study there are 90 reference points divided into 1) 30 points of burned area, 2) 30 points of non-burned areas, and 3) 30 points of forest areas. A random point was created in the ArcGIS program.

RESULTS AND DISCUSSIONS

FCC for Investigating Forest Fire Burned Areas

The April 2021 data from Landsat 8 OLI were created in false color composite (FCC) SWIR-NIR-Red (RGB: 754) wavelength range. Forest fire burned areas were shown clearly as seen in Figure-1.

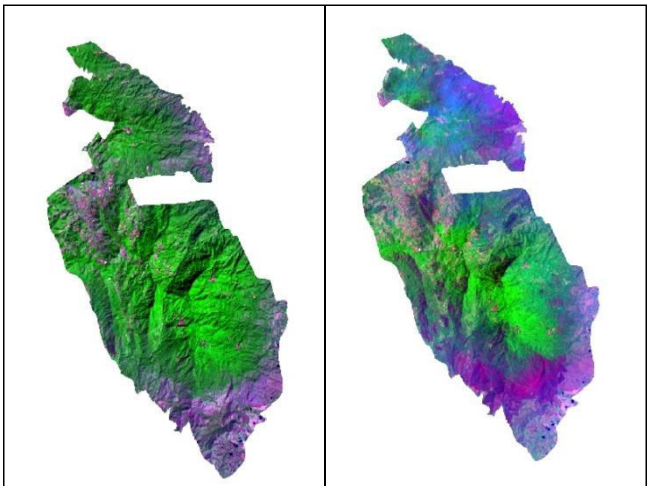

(a) Before forest fires b) after forest fires

Figure-1. A forest fire burned areas a) Before forest fires and b) after forest fires.

In Figure-1 (b), Severe forest fire burned areas appear in purple or dark purple, and small burned areas appear in light purple. Forest areas appear in green and light green or dark green, depending on the types of vegetation, tree phenology, and density of plants that cover the soil. The result obtained from FCC, SWIR-NIR-Red (RGB:754) in April 2021 was analyzed to make a comparison and investigate forest fire burned areas to spectral indices analysis; NDVI, NBR, and BAI. There are 100 reference points. The comparative analysis result is shown in Figures 2-4.

VOL. 18, NO. 9, MAY 2023 ISSN 1819-6608
ARPN Journal of Engineering and Applied Sciences

www.arpnjournals.com

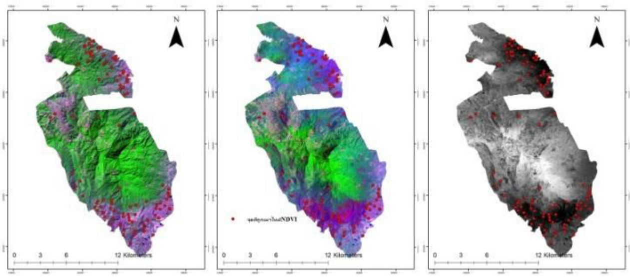

(a) (b) (c)

Figure-2. Comparison and investigate forest fire burned areas of NDVI (a) Before forest fires**,** (b) after forest fires and (c) NDVI.

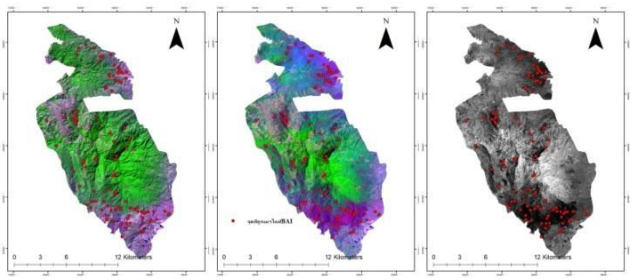

(a) (b) (c)

Figure-3. Comparison and investigate of forest fire burned areas of BAI (a) Before forest fires**,** (b) after forest fires and (c) BAI.

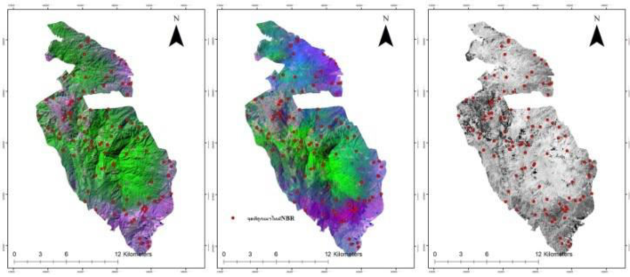

(a) (b) (c)

Figure-4. Comparison and investigate forest fire burned areas of NBR (a) Before forest fires**,** (b) after forest fires and (c) NBR.

From Figures 2-4, it was found that in April 2021, based on visual interpretation point by point, NDVI had 80 out of 100 points of burned area, accounting for 80%, BAI had 91 out of 100 points of burned area, accounting for 91% and NBR had 67 out of 100 points of burned area, accounting for 67%.

Accuracy Evaluation

The Landsat 8 OLI data analysis result was evaluated accuracy using Kappa statistic, including results from the analysis of false color composite (FCC**,** SWIR-NIR-Red (RGB:754) in April 2021, spectral indices analysis; NDVI, NBR, and BAI in April 2021 which 90 reference points were determined and created a random point in ArcGIS. 90 reference points are divided into 1) 30 points of burned area, 2) 30 points of non-burned area, and 3) 30 points of forest area. Accuracy evaluation can be described according to Table-2 to Table-4.

Table-2. Accuracy evaluation of NDVI.

∆NBR	Forest area	Non-forest area	Burning area	Sum	User's Accuracy
Forest area	23	4	3	30	76.67%
Non-forest area	2	20	8	30	66.67%
Burning area	4	7	19	30	63.33%
Sum	29	30	31	90	
Producer's accuracy	79.31%	66.67%	61.29%		
Kappa statistics	0.77				

ARPN Journal of Engineering and Applied Sciences

Table-3. Accuracy evaluation of BAI.

∆NBR	Forest area	Non-forest area	Burning area	Sum	User's Accuracy
Forest area	25	2	3	30	83.33%
Non-forest area	4	24	2	30	80%
Burning area	2	2	26	30	86.67%
Sum	31	28	26	90	
Producer's accuracy	80.65%	85.71%	83.87%		
Kappa statistics	0.87				

Table-4. Accuracy evaluation of NBR.

∆NBR	Forest area	Non-forest area	Burning area	Sum	User's Accuracy
Forest area	18	7	5	30	60%
Non-forest area	6	16	8	30	53.33%
Burning area	6	8	16	30	53.33%
Sum	30	31	29	90	
Producer's accuracy	60%	51.61%	55.17%		
Kappa statistics	0.67				

From Table-2 (NDVI), according to overall accuracy, it was found that the Kappa coefficient (Kappa Statistics) of consistency was 0.77. Consideration of a class of burned area found that the producer's accuracy was 61.29 %, omission error was 38.71%, users' accuracy was 63.33% and commission error was 63.33 %.

From Table-3 (BAI), according to overall accuracy, it was found that the Kappa coefficient (Kappa Statistics) of consistency was 0.87. Consideration of a class of burned area found that the producer's accuracy was 83.87%, omission error was 16.12%, users' accuracy was 86.67% and commission error was 13.33%.

From Table-4 (NBR), according to overall accuracy, it was found that the Kappa coefficient (Kappa Statistics) of consistency was 0.67. Consideration of a class of burned area found that the producer's accuracy was 55.17 %, omission error was 44.83%, users' accuracy was 53.33% and commission error was 46.67%.

CONCLUSIONS

Forest fires are considered a disaster. Once it occurs, it causes huge damage. Forest fires can occur due to natural reasons, such as lightning, volcanic eruptions, extremely hot weather, drought, and human activities like hunting and gathering forest products, burning farms, and raising livestock. This study aims to apply remote sensing technology using data from Landsat 8 OLI to investigate areas burned by forest fires in Doi Suthep-Pui National Park, Chiang Mai province. The difference of spectral indices in 4 patterns are used, i.e. Normalized Difference Vegetation Index (NDVI), Normalized Burned Ratio (NBR), and Burn Area Index (BAI) in April 2021. According to the study results, it can be concluded that BAI gave the highest accuracy for the investigation of forest fire-burned areas, followed by NDVI, BAI, and NBR. The comparison values of forest fire-burned areas account for 77%, 87%, and 67% respectively. Besides, accuracy measured by Kappa statistics indicated that BAI gave the highest accuracy for the investigation of forest fire burned areas as Kappa statistic was 0.87, followed by NDVI showing Kappa statistic equal to 0.77, NBR showing Kappa statistic equal to 0.67. In addition, the data analysis, based on the false color composite (FCC) method, SWIR-NIR-Red (RGB: 754), revealed spatial data, especially forest fire-burned areas that appear in dark purple. Preparation or planning made by existing resources shall be able to prevent and cope with forest fires in an efficient manner.

ACKNOWLEDGEMENTS

This research project is financially supported by Mahasarakham University.

REFERENCES

Chiang Mai Provincial Office. 2021. Briefing Chiang Mai Province. Available online: https:// www.chiangmai.go.th/managing/public/D8/8D12Nov2020 103220.pdf. (accessed on 20 March 2022).

Department of National Parks, Wildlife and Plant Conservation. 2019. Thailand Forest Fire Statistics. Available online: http://www.dnp.go. th/forest fire/web/frame/statistic.html (accessed on 25 December 2019).

Department of National Parks, Wildlife and Plant Conservation. (n.d.). Policies and Ideas for Solving Forest Fire Problems. Available online: https://www.dnp.go.th/forestfire/firescience/lesson%202/lesson21.htm/ (accessed on 15 March 2022).

Elachi C., Zyl J. V. 2021. Introduction to the Physics and Techniques of Remote Sensing (3rd Edition). John Wiley & Sons, Inc.

ESA. 2016. Physics of Remote Sensing. Available online: https://earth.esa.int/web/eo-summer-school/documents/973910/2642313/JG1to3.pdf (accessed on 15 June 2022).

Filipponi F. 2018. BAIS2: Burned Area Index for Sentinel-2. Proceedings. 2(7): 364.

Jomsrekrayom N., Meena P., Laosuwan T. 2021. Spatiotemporal Analysis of Vegetation Drought Variability in the Middle of the Northeast Region of Thailand using Terra/Modis Satellite Data. Geographia Technica. 16(Special Issue): 70-81.

Keeley J. E. 2009. Fire intensity, fire severity and burn severity: A brief review and suggested usage. International Journal of Wildland Fire. 18(1): 116-126.

Kongmeesup I. 2020. Interactions between Climate Change and the World's Forest Sector. Naresuan Agricultural Journal. 17(2): 1-19.

Laosuwan T. and Uttaruk P. 2014. Estimating Tree Biomass via Remote Sensing, MSAVI 2, and Fractional Cover Model. IETE Technical Review. 31(5): 362-368.

Laosuwan T., Sangpradid A., Gomasathit T., Rotjanakusol T. 2016. Application of remote sensing technology for drought monitoring in Mahasarakham Province, Thailand. International Journal of Geoinformatics. 12(3): 17-25.

Linta N., Mahavik, N., Chatsudarat, S., Seejata K. and Yodying A. 2021. Analysis of Burning Area from Forest Fire using Sentinel-2 Image: A Case Study of Pai, Mae Hong Son Province. Journal of Applied Informatics and Technology. 3(2): 101-121.

Prohmdirek T., Chunpang P. and Laosuwan T. 2020. The Relationship between Normalized Difference Vegetation Index and Canopy Temperature that Affects the Urban Heat Island Phenomenon. Geographia Technica. 15(2): 222-234.

Rouse J. W., Haas R. H., Schell J. A. and Deering D. W. 1973. Monitoring vegetation systems in the Great Plains with ERTS (earth resources technology satellite). In: Third Earth Resources Technology Satellite Symposium. Greenbelt, ON, Canada. 10-14/12/1973, 309-17.

Rotjanakusol T. and Laosuwan T. 2018. Estimation of land surface temperature using Landsat satellite data: A case study of Mueang Maha Sarakham District, Maha Sarakham Province, Thailand for the years 2006 and 2015. Scientific Review - Engineering and Environmental Sciences. 27(4): 401-409.

Rotjanakusol T. and Laosuwan T. 2018. Inundation area investigation approach using remote sensing technology on 2017 flooding in Sakon Nakhon province Thailand Studia Universitatis Vasile Goldis Arad, Seria Stiintele Vietii. 28(4): 159-166.

Rotjanakusol T. and Laosuwan T. 2019. An Investigation of Drought around Chi Watershed during Ten-year Period using Terra/modis Data. Geographia Technica. 14(2): 74-83.

Rotjanakusol T. and Laosuwan T. 2019. Drought Evaluation with NDVI-based Standardized Vegetation Index in Lower Northeastern Region of Thailand. Geographia Technica. 14(1): 118-130.

Rotjanakusol T. and Laosuwan T. 2020. Model of Relationships between Land Surface Temperature and Urban Built-Up Areas in Mueang Buriram District, Thailand. Polish Journal of Environmental Studies. 29(5): 3783-3790.

Rotjanakusol T. and Laosuwan T. 2020. Surface Water Body Extraction Using Landsat 8 Images and Different Forms of Physical Models. Scientific Journal of King Faisal University: Basic and Applied Sciences. 21(2): 218-223.

Ruthamnong S. 2019. Burned area extraction using Multitemporal Difference of Spectral Indices from Landsat 8 Data: A case study of Khlong Wang Chao, Klong Lan, and Mae Wong National Park. The Golden Teak: Humanity and Social Science Journal. 25(2): 49-65.

Suriya W., Chunpang P., Laosuwan T. 2021. Patterns of the relationship between PM10 from air monitoring quality station and AOT data from MODIS sensor onboard of Terra satellite. Scientific Review Engineering and Environmental Sciences. 30(2): 236-249.

Thai National Parks. 2022. Doi Suthep-Pui National Park. Available online: https://www.thainational parks.com/doi-suthep-pui-national-park (accessed on 20 August 2022).

The University of Lucknow. (n.d.). Physics of Remote Sensing. Available online: https://www.lkouniv.ac.in/site/writereaddata/siteContent/202004021910156883 ajay_misra_geo_principles_of_RS.pdf (accessed on 12 June 2022).

U. S. Geological Survey. 2020. Landsat 8-9 Operational Land Imager (OLI) - Thermal Infrared Sensor (TIRS) Collection 2 Level 2 (L2) Data Format Control Book (DFCB). Available online: https://earth.esa.int/eogateway/documents /20142/0/Landsat-8-9-OLI-TIRS-Collection-2-Level-2-Data-Format-Control-Book-DFCB.pdf (accessed on 02 May 2022).

Uttaruk Y., Rotjanakusol T., Laosuwan T. 2022. Burned Area Evaluation Method for Wildfires in Wildlife Sanctuaries Based on Data from Sentinel-2 Satellite. Polish Journal of Environmental Studies. 31(6): 5875-5885.

Xiao C., Li P. and Feng Z. 2019. A renormalized modified normalized burn ratio (RMNBR) index for detecting mature rubber plantations with Landsat-8 OLI in Xishuangbanna, China. Remote Sensing Letters. 10(3): 214-223.